



## Gas pixel detector for X-ray observation

D. Attié<sup>a,\*</sup>, M. Campbell<sup>b</sup>, M. Chefdeville<sup>c</sup>, P. Colas<sup>a</sup>, E. Delagnes<sup>a</sup>, Y. Giomataris<sup>a</sup>, H. van der Graaf<sup>c</sup>, X. Llopart<sup>b</sup>, J. Timmermans<sup>c</sup>, J. Visschers<sup>c</sup>

<sup>a</sup> CEA, Irfu, SPP, Centre de Saclay, F-91191 Gif-sur-Yvette, France

<sup>b</sup> CERN, CH-1211 Genève 23, Switzerland

<sup>c</sup> NIKHEF, Kruislaan 409, Amsterdam 1098 SJ, The Netherlands

### ARTICLE INFO

Available online 13 June 2009

#### Keywords:

Diffusion in gases  
Electronic circuits  
Microelectronics  
Gas-filled counters  
Photolithography  
Photon counting and statistics  
Polarimeters  
X-ray detectors

### ABSTRACT

We report on the status of the R&D for a digital Time Projection Chamber (TPC) based on Micromegas (*MICRO MESH Gaseous Structure*) detectors using the CMOS chip TimePix as a direct readout anode protected by highly resistive a-Si:H layer. A small chamber was built as a demonstrator of the 2-D and 3-D imaging capabilities of this technique. We illustrate the new capabilities of this detector for X-ray observation with data taken from radioactive sources. This small TPC is a very useful tool both for studying gas properties thanks to its good efficiency for single electrons, and for reconstructing photoelectron direction for use as a soft X-ray polarimeter.

© 2009 Elsevier B.V. All rights reserved.

## 1. Introduction

By the recent advancement in microelectronics, the pixel readout chip technology achieved a granularity of a few tens of microns. When combined with a micro-pattern gas detector, such as Micromegas (*MICRO MESH Gaseous Structure*), for electron amplification [1], each pixel is sensitive to a single primary gas electron [2]. This ensures the ultimate spatial resolution for tracking images. Such a detector can also be used for soft X-ray observation ( $1 \text{ keV} < E_\gamma < 50 \text{ keV}$ ).

After introducing the advantages of a digital Time Projection Chamber (TPC) we describe our prototype based on TimePix readout chips and Micromegas detectors. Afterwards we present two applications for X-ray observation: studies of primary electron statistics in gases and soft X-ray polarimetry or for high energy physics experiments.

## 2. Digital TPC based on TimePix and Micromegas

### 2.1. Advantages of a pixelized gas detector

Gas and solid detectors are able to collect and amplify the electrons released by ionizing radiation. But the gas medium has the advantage to affect less the incident radiation than the solid detector. Additionally, a pixelized detector provides a high granularity single electron sensitive readout which yields the

ultimate spatial resolution. Gaseous trackers are sensitive to both minimally ionizing particles and photoelectric events on account of longer radiation lengths.

The incident particles interacts with the gas medium and produce electron–ion pairs. These pairs are separated by the electric field (a few hundred V/cm) and the electrons drift towards the anode plane. Thus, the electrons from ionization are projected on the readout plane providing 2-D localization. The information of the third dimension is given by the arrival time of the electrons, if the creation time and drift velocity is known. The total primary charge can be recorded to measure the energy lost by the incoming particles. For many applications, the pixelized gas detector is an excellent 2-D and 3-D imaging device with high spatial resolution.

### 2.2. Digital micro-TPC prototype

Fig. 1 shows the exploded view of the small detector we built as a digital TPC prototype. The detector consists of an aluminum chamber containing a field cage ( $2 \times 2 \times 6 \text{ cm}^3$ ) mounted on a frame which holds a  $50 \mu\text{m}$  gap Micromegas mesh on top of the chip. The field cage is folded kapton with 15 copper strips (4 mm pitch, 3 mm width), between each is a  $1 \text{ M}\Omega$  resistor to provide a uniform electric field. The TimePix chip and the Micromegas detector are described in the two following sections.

#### 2.2.1. TimePix chip

TimePix is a pixel readout chip designed in  $0.25 \mu\text{m}$  CMOS ASIC technology which contains a square matrix of  $256 \times 256$  pixels, each  $55 \times 55$  microns [3]. Each pixel has a low noise

\* Corresponding author.

E-mail address: [david.attie@cea.fr](mailto:david.attie@cea.fr) (D. Attié).

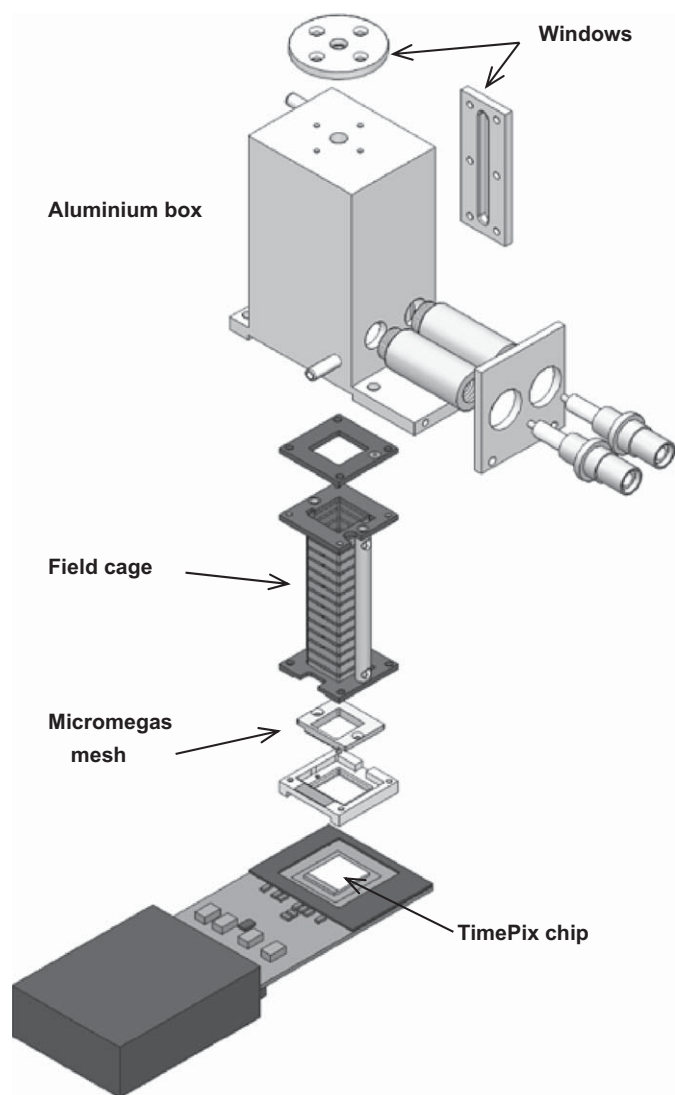


**Fig. 1.** Exploded view of Micro-TPC formed by a 6 cm field cage placed on the TimePix chip inside a small aluminium chamber.

preamplifier-shaper, a discriminator, a threshold DAC, a 14-bit counter and a TimePix Synchronization Logic (TSL) circuit. Each pixel can be independently set in one of five different modes (masked, hit counter, time-over-threshold (TOT), time and one-hit time). The TSL was designed to count clock pulses up to 100 MHz. During a user-defined time window (shutter time), every pixel that detects a signal crossing the threshold counts clock pulses unless it is masked; while the signal is above the threshold (*time-over-threshold* mode); or until the end of the shutter time (*time* mode). The *time-over-threshold* mode gives information regarding the total avalanche charge for each pixel, while the *time* (or *Timepix*) mode provides the electron arrival time.

The TimePix chip, based on Medipix2 chip [4], was designed for radiation tracking in gases for TPC applications.

### 2.2.2. Micromegas and chip protection

Micromegas is an amplification system using a thin metal mesh held above the anode plane by pillars of 50–150  $\mu\text{m}$  height. The gas gain occurs when incoming electrons multiply creating an avalanche in the strong electric field between the mesh and the anode, due to an applied potential difference [5]. In typical working conditions, the avalanche size is approximately 15  $\mu\text{m}$

rms assuring that one electron avalanche is collected on only one given pixel.

Post-processing technology makes it possible to integrate a Micromegas structure directly onto the chip (InGrid). The InGrid holes can be aligned precisely with the pixel pads while the pillar diameter can be made small enough ( $\approx 20 \mu\text{m}$ ) to be placed between the holes [6].

In order to protect the chip against destructive sparks, a 20  $\mu\text{m}$  thick highly resistive a-Si:H layer was deposited onto the chip by a plasma process at  $\approx 200^\circ\text{C}$  [7]. This protective cover, called *SiProt*, has a resistivity of  $10^{11} \Omega\text{cm}$  and intends to protect the chip from high instantaneous spark currents which could destroy the chip.

## 3. Applications for X-ray observation

### 3.1. Measurements of primary statistics in gases

In gas detectors, the spatial resolution  $\sigma_t$  is mainly determined by the electron diffusion, which can be described by factor  $\sqrt{2 \cdot D \cdot t}$ , where  $D$  is the electron diffusion coefficient. This coefficient  $D$  depends of the gas mixture and the electric field. To measure the number of primary electrons produced by soft X-ray photons we used the digital Micro-TPC filled with Argon(95%)–Isobutane(5%). In this mixture, which has a large transverse diffusion coefficient  $D_t$ , the primary electrons from the  $^{55}\text{Fe}$ 's 5.9 keV photons are imaged into isolated clusters of 1–3 pixels (Fig. 2, left). Currently *SiProt* spreads by induction the electron avalanche over several pixels. Fig. 3 shows the spectrum of number of electrons for 2000 events (photons) using an InGrid on top of a TimePix chip covered with 15  $\mu\text{m}$  of *SiProt*. The transverse diffusion coefficient  $D_t$  is  $500 \mu\text{m}/\sqrt{\text{cm}}$  at 500 V/cm in Argon(95%)–Isobutane(5%). The spectrum has been fitted by two Gaussians to account for the  $K_\alpha$  and  $K_\beta$  lines. The mean of the  $K_\alpha$  line corresponds to the specific number of electrons converted in this gas mixture (226 electrons). The measured energy resolution  $\sim 4\%$ , defined as full width half maximum divided by peak position of the response function, shows that the electron number distribution is sub-poissonian as expected from Fano theory. The energy resolution obtained using electron counting is slightly better than the energy resolution obtained when reading out the grid signal which is about 5% (rms). With an acquisition time of 100  $\mu\text{s}$ , background from noise hits can be suppressed using the electrons arrival time which allows a very low detection threshold and thus a single electron efficiency ( $> 90\%$ ) (Fig. 2, left). Some preliminary results show that the mean value corresponds to 232 electrons converted in the Argon(95%)–Isobutane(5%) gas mixture at an efficiency near 100%.

### 3.2. Polarimetry using photoelectric absorption

Photoelectric X-ray polarimetry with gas-based detectors was first demonstrated in 1923 using a Wilson chamber [8] and recently by micro-pattern gas detectors using a gas electron multiplier [9,10]. They achieved a quantum efficiency up to 6% at 6.4 keV.

The technique consists in determining the emission angle of the photoelectron by imaging its track in a gas medium.

This puts constraints on the gas mixture. On the one hand it should have enough absorption length to retain a good detection efficiency for few-keV X-rays, on the other hand, the diffusion limits the ability to measure the angle of the photoelectron. As a compromise, we choose a gas mixture of Neon(90%)–Isobutane(10%) (electron transverse diffusion coefficient  $D_t \approx 350 \mu\text{m}/\sqrt{\text{cm}}$ ) and a

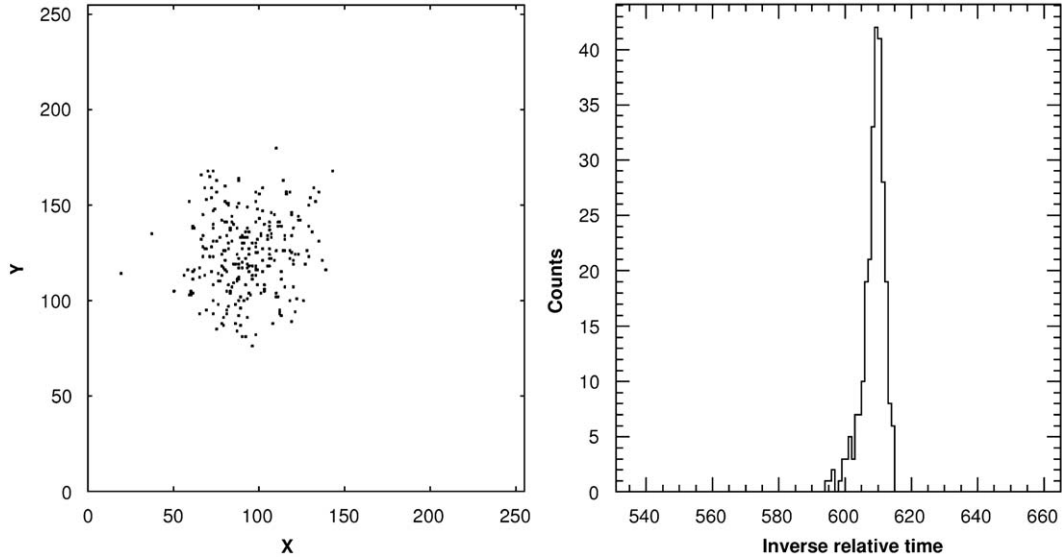


Fig. 2. Cluster of electrons from an X-ray photon <sup>55</sup>Fe source converted in Argon(95%)–Isobutane(5%) gas mixture (left) and its corresponding time spectrum (right). A selection in time helps to suppress the background.

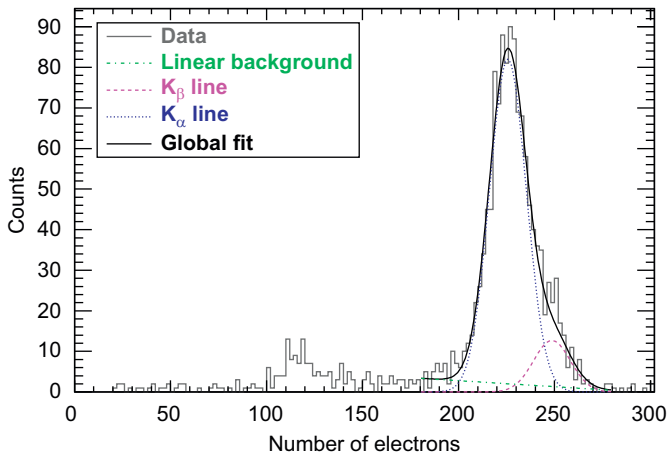


Fig. 3. Spectrum of the number of electrons obtained with each of 2000 photons from <sup>55</sup>Fe source converted in Argon(95%)–Isobutane(5%) gas mixture. The  $K_\alpha$  and  $K_\beta$  lines have been fitted by two Gaussians. The mean of the line is 226 electrons and the RMS  $\simeq 4\%$ . The electron transverse diffusion coefficient was  $D_t = 500 \mu\text{m}/\sqrt{\text{cm}}$  at 500 V/cm.

drift distance of 5 mm. With this gas mixture the 5.9 keV photons absorption is 2.2%.

The photoelectric effect has a large cross-section at low energy making the process very sensitive to photon polarization. In the non-relativistic limit, the angular dependence of the differential cross-section is given by

$$\frac{d\sigma}{d\Omega} \propto \frac{\sin^2 \theta \cos^2 \phi}{(1 - \beta \cos \theta)}$$

where  $\beta = v/c$  is the electron velocity,  $\phi$  is the polarization-dependent azimuthal angle, and  $\theta$  is the polar angle with respect to the incident photon momentum (see Fig. 4). For linearly polarized photons, the differential photoelectron cross-section has a maximum probability ( $\theta = 0$ ) in the plane orthogonal to the direction of the electric field of the incident photon with a  $\cos^2 \phi$  modulation. The polarization signature is given by the photoelectron angle distribution  $N(\phi) = A + B \cos^2(\phi - \phi_{pol})$  and

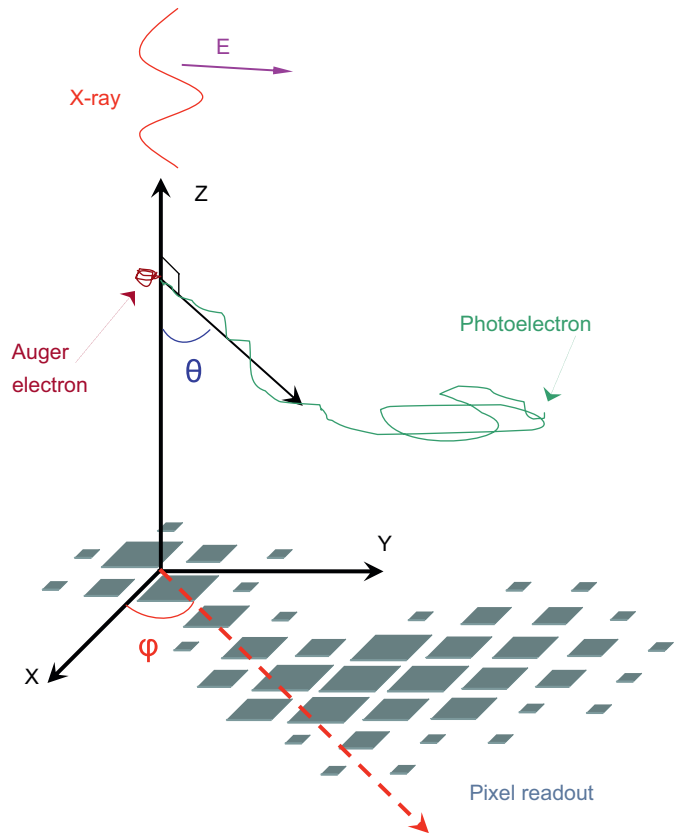


Fig. 4. Angular distribution and projection on the pixel readout of the detector plan (XY) obtained by an ejected photoelectron.

the modulation factor of a 100% linearly polarized radiation is

$$\mu = \frac{N_{\max} - N_{\min}}{N_{\max} + N_{\min}} = \frac{B}{2A + B}$$

Using our digital TPC, with a drift distance of 5 mm, the photoelectron ejected after the absorption of <sup>55</sup>Fe photon in the gas volume produces a track of electrons. The 55  $\mu\text{m}$  pixel readout

chip allows a 2-D reconstruction of the photoelectron track ( $\approx 1$  mm).

The direction of emission of the photoelectron could be reconstructed by finding in first approximation the principal axis of the charge distribution on the pixels set in TOT mode (Fig. 5). The track image also contains information on the dynamics of the photoelectron energy loss; in case of asymmetric charge distribution, where the photoelectron track is seriously affected by Coulomb scattering, a better reconstruction of the photoelectron angle is possible by evaluating the absorption point after removing the final part of the track [11].

#### 4. Summary

The principle of pixel gas detector has been demonstrated by combining Micromegas with the TimePix readout chip and resistive layer for protection. Beside the 3-D imaging capability, this small chamber is a very well suited for studying gas properties such as gain fluctuation and primary electron statistics. It could also be used as a soft X-rays polarimeter due to its ability to measure energy and directionality of photoelectrons with high spatial resolution, however with efficiency at a few percent level.

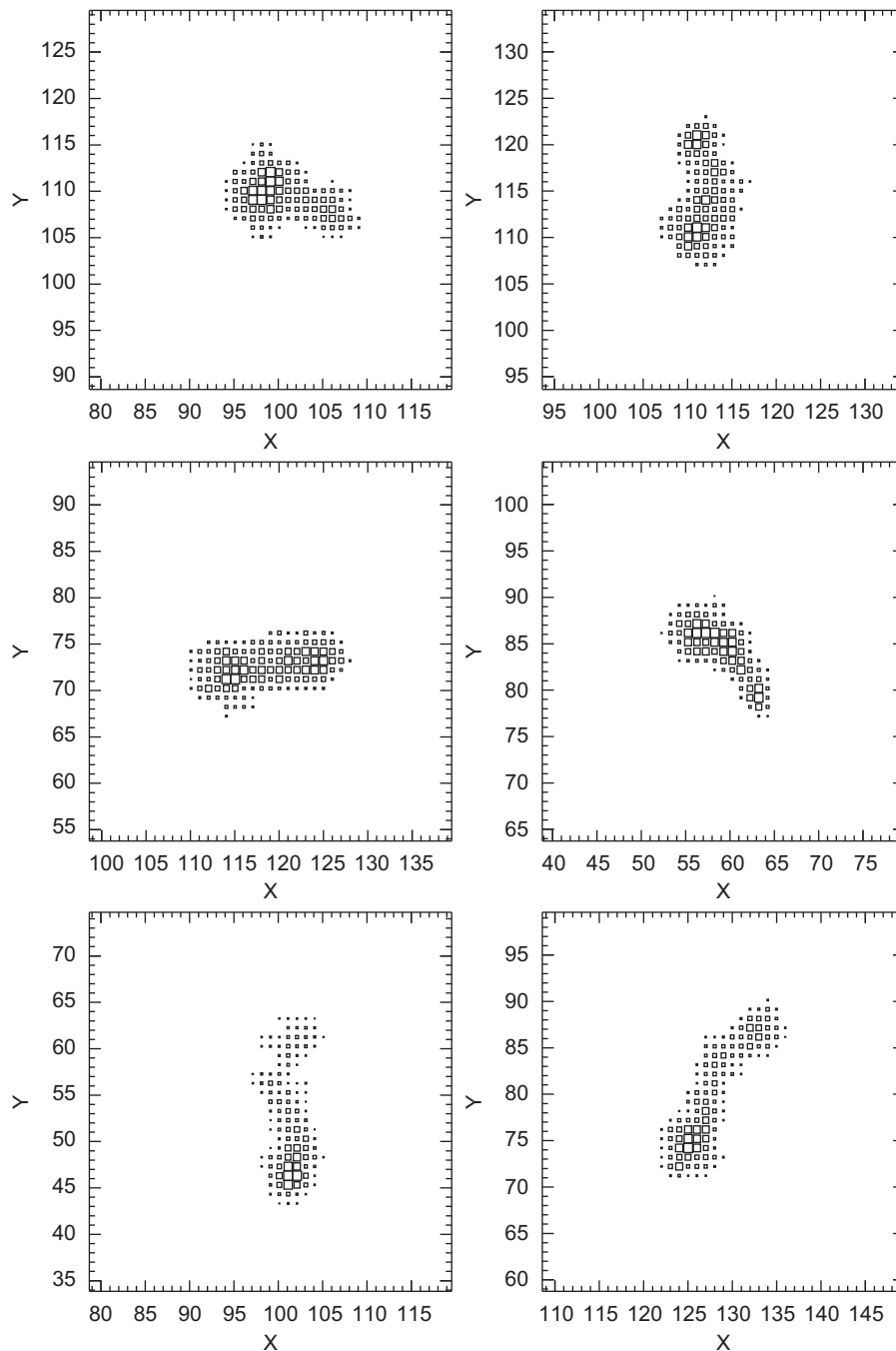


**Fig. 5.** Examples of photoelectron tracks ( $\approx 1$  mm) obtained with the 5.9 keV X-rays from  $^{55}\text{Fe}$  in Neon(90%)–Isobutane(10%) and a drift distance of 5 mm. The area of each square is proportional to the charge collected by the corresponding pixel set in TOT mode. The size of each image is 2.2 mm (40 pixels).

## Acknowledgments

This work is supported by the Commission of the European Communities under the 6th Framework Programme “Structuring the European Research Area”, Contract number RII3-026126. We also thank the organizers of the 5th International Conference on New Developments In Photodetection 2008 for giving us the opportunity to present this work.

## References

[1] P. Colas, et al., Nucl. Instr. and Meth. A 535 (2004) 506.

- [2] M. Campbell, et al., Nucl. Instr. and Meth. A 540 (2005) 295.
- [3] X. Llopert, et al., Nucl. Instr. and Meth. A 581 (2007) 485.
- [4] X. Llopert, et al., IEEE Trans. Nucl. Sci. NS-49 (2002) 2279.
- [5] Y. Giomataris, et al., Nucl. Instr. and Meth. A 376 (1996) 29.
- [6] M. Chefdeville, et al., Nucl. Instr. and Meth. A 556 (2006) 490.
- [7] N. Wyrsh, et al., in: Proceedings of the MRS Symposium, vol. 869, 2005, pp. 3–14.
- [8] C.T.R. Wilson, R. Soc. Proc. A 85 (1923) 1.
- [9] R. Bellazzini, et al., Nucl. Instr. and Meth. A 572 (2007) 160.
- [10] J.K. Black, et al., Nucl. Instr. and Meth. A 581 (2007) 755.
- [11] R. Bellazzini, et al., Nucl. Instr. and Meth. A 510 (2003) 176.